



The superprism effect using large area 2D-periodic photonic crystal slabs

S.N. Tandon^{*}, M. Soljačić, G.S. Petrich, J.D. Joannopoulos, L.A. Kolodziejski

Research Laboratory of Electronics, 77 Massachusetts Avenue Room 36-295, Massachusetts Institute of Technology, Cambridge, MA 02139-4307, USA

Received 22 January 2005; received in revised form 2 March 2005; accepted 18 May 2005
Available online 13 June 2005

Abstract

The “superprism effect” is an effect observed in photonic crystal structures whereby the direction of light propagation is extremely sensitive to the wavelength and angle of incidence. To realize the superprism effect, new structures are presented which rely on the sensitivity of the phase velocity in a two-dimensional (2D) photonic crystal slab to observe angular magnification outside the photonic crystal medium. Constant frequency contour calculations for a photonic crystal slab of finite thickness are used to predict the phase velocity superprism effect. Further analysis using 2D finite-difference time-domain simulations indicate that a large area photonic crystal and wide excitation beam are necessary for clear observation of the superprism effect. A fabrication technique is demonstrated to achieve the structure’s required nanometer-sized features over centimeter-scale areas.

© 2005 Elsevier B.V. All rights reserved.

PACS: (42.70.Qs) Photonic bandgap materials; (42.82.-m) Integrated optics; (42.82.Cr) Fabrication techniques

Keywords: Photonic crystals; Superprism effect; Interference lithography

1. Introduction

The “superprism effect” is one example of the unique behavior of light in photonic crystals. A photonic crystal allows the creation of a “superprism” which behaves similarly to a conventional prism only with greatly enhanced sensitivities with respect to the wavelength and direction of incident light, termed: (1)

super-dispersion and (2) angular magnification, respectively. Just as a conventional prism separates multiple wavelength components of incident light to form a “rainbow,” a superprism will separate the wavelengths over much wider angles resulting in “super dispersion.” Alternatively, for a single wavelength light beam, a small tilt in the incident angle will result in a much larger change in the propagation direction of the outgoing beam. Thus a superprism can be used to magnify the angular range of a single wavelength of light to steer a beam over wider angles; this second property is termed “angular

^{*} Corresponding author. Tel.: +1 617 253 2488; fax: +1 617 253 8509.

E-mail address: tandon@mit.edu (S.N. Tandon).

magnification.” Being able to realize the enhanced effects of a superprism would be very useful for a number of applications ranging from new devices for wavelength-division-multiplexed (WDM) systems to a new class of optical elements for beam manipulation within integrated optical circuits. Spectral separation and beam steering functions are more compactly controlled using a single superprism device rather than a larger system composed of prisms, lenses, and mirrors.

A material can influence the propagation of light by affecting its *group velocity* and/or *phase velocity* characteristics. The group velocity is a vector which indicates the direction of energy propagation ($\mathbf{v}_g = \nabla_{\mathbf{k}}\omega$), while the phase velocity is a scalar whose value ($v_p = \omega/|\mathbf{k}|$) is the “speed of light,” or the speed of the electromagnetic phase within a material. The vector \mathbf{k} ($|\mathbf{k}| = 2\pi/\lambda$) indicates the direction in which the phase fronts propagate. In uniform isotropic materials, the group velocity and the \mathbf{k} -vector point in the same direction and are dependent on orientation and frequency. For example, inside a conventional glass prism, a spectrum of colors diverges due to the frequency dependence of the phase and group velocities. By creating a periodic variation in the index of refraction of a material to form a “photonic crystal,” the group velocity and phase velocity characteristics of light can be engineered for a much stronger dependence on frequency or orientation. As a result, photonic crystals (PCs) are at the heart of the superprism effect. In addition, because the group velocity and \mathbf{k} -vector in a PC can point in very different directions, the conditions in which the group velocity is highly sensitive to orientation and wavelength can differ from the conditions in which phase velocity is sensitive to orientation and wavelength.

A number of groups have previously designed and fabricated superprism devices using different photonic crystal designs [1–5]. The common theme between these groups is that they have utilized sensitivity of the *group velocity*, to accomplish either angular magnification or super dispersion. The photonic crystals utilized by these groups were designed to exhibit large changes in the group velocity for small changes in wavelength or orientation. Kosaka, et al. used a three-dimensional (3D) photonic crystal to demonstrate both super dispersion and angular magnification based on the

directional and spectral sensitivity of the group velocity within the PC [1,2]. Large changes in beam direction within the photonic crystal were demonstrated for small changes in both angle and wavelength. Alternatively, to circumvent the fabrication complexities associated with the 3D superprism, Nelson, et al. demonstrated that strong wavelength dispersion effects can be achieved using a simpler one-dimensional PC composed of multiple GaAs/AlGaAs layers [3]. Wu, et al. also used group velocity effects to demonstrate that a 2D photonic crystal of air holes in GaAs can be used to observe superprism effects using a planar configuration [4]. Wu, et al. relied on the group velocity sensitivity to change the direction of the beam as the incident wavelength changes. With a silicon-on-insulator (SOI) layered structure, Lupu, et al. also demonstrated that group velocity effects within a 2D photonic crystal slab allow small changes in wavelength to significantly alter a beam’s direction [5].

Each of the aforementioned reports have shown that photonic crystals can be used to greatly alter the propagation angle of light *while traveling within the photonic crystal*. To maintain the angular effect when light exits the photonic crystal or a region containing the photonic crystal, group velocity sensitivity is not sufficient. While the sensitivity of the group velocity within a photonic crystal can allow significant bending of light within the PC, the phase velocity determines the angle of propagation when light exits the PC and enters a uniform material. In uniform materials, the propagation angle is calculated using Snell’s Law, whereas in photonic crystals, the propagation angle depends on the band structure. In general, the propagation angle after any interface is determined by a boundary condition which requires the tangential component of the \mathbf{k} -vector to remain constant. Since the phase velocity is related to the \mathbf{k} -vector through $v_p = \omega/|\mathbf{k}|$, while the group velocity is related through a derivative, the phase velocity directly determines the behavior of light at the boundary. With a large change in the group velocity, combined with no change in the phase velocity, the beam’s position only experiences a spatial translation with no change in its angular properties. In other words, the beam “refracts back” to its original angle of incidence at the input upon exiting the structure.

In this paper, a superprism structure is designed using a large area two-dimensionally periodic photo-

nic crystal slab such that angular magnification can be observed in an output slab of *uniform material*. The superprism effect explored in this work relies on angular sensitivity of the phase velocity rather than sensitivity of the group velocity. By affecting the angular dependence of the phase velocity, the enhanced effects introduced by the photonic crystal are preserved as the beam propagates out of the photonic crystal into uniform material. An additional advantage of the phase velocity approach is that the photonic crystal can be terminated along lines of symmetry, thereby avoiding scattering effects normally associated with photonic crystal structures of other terminations. To demonstrate the feasibility of the phase velocity-dependent superprism approach, the relevant equi-frequency curves are calculated with a 3D eigen-frequency solver [6]. Finite-difference time-domain (FDTD) simulations [7] of a 2D model are also performed. The 2D calculations indicate that a wide excitation beam approximating a plane wave, is necessary for clearly observing the angular magnification property of the superprism. As a result, the superprism structure containing a large area photonic crystal is required to allow the wide beam to propagate through the photonic crystal. A technique for fabricating the large area 2D slab structure has also been explored using interference lithography to pattern nanometer-sized features over centimeter-scale areas.

2. Theory

The superprism structure described herein was designed to use a photonic crystal to observe angular magnification as light enters a uniform medium. Therefore, the photonic crystal slab was designed such that large changes in the phase velocity (and \mathbf{k} -vector) are created for small changes in the angle of incidence as suggested by Luo, et al. [8] and Baba, et al. [9]. A convenient way to analyze the directional dependence of the \mathbf{k} -vector within the photonic crystal is by calculating and plotting a dispersion surface. The dispersion surface, also known as an equi-frequency surface, maps out the allowed \mathbf{k} -vectors for all orientations within a structure for a constant frequency. In a uniform isotropic material, where the phase and group velocities are independent of

orientation, the dispersion surface is a circle. The radius of the circle is the magnitude of the \mathbf{k} -vector, which scales with the phase velocity, and the group velocity points away from the circle in the direction normal to the surface. However, in photonic crystals, due to the periodicity in the refractive index, neither the phase velocity nor group velocity are constant and depend on direction. Hence, the dispersion surface is no longer circular.

A dispersion surface with low curvature regions is ideal for creating a superprism effect where large changes in the phase velocity occur for small changes in direction. In contrast, dispersion surfaces with regions of high curvature are ideal for creating a large group velocity change for a small shift in orientation. Fig. 1 presents the calculated dispersion surfaces associated with a number of frequencies for the structure shown. The structure consists of a photonic crystal slab with a square lattice of air holes in the top silicon layer of a silicon-on-insulator wafer. The dispersion surfaces are presented as a function of normalized frequency and scale linearly with wavelength. The photonic crystal has a lattice constant a , a hole radius $r = 0.4a$, a silicon layer thickness $t_{\text{Si}} = 14a/15$, and an underlying SiO_2 layer thickness $t_{\text{ox}} = 4a$. The “flattest” dispersion surface occurs at a normalized frequency of $fa/c = 0.22$ suggesting that superprism operation will occur at this frequency. The lattice constant is then chosen to be $a = 0.22\lambda_{\text{air}}$ based on the desired operating wavelength.

The superprism phenomenon expected from the relevant dispersion surface ($fa/c = 0.22$) in Fig. 1, is illustrated in Fig. 2. A schematic of the light path through the entire photonic crystal with input and output interfaces is shown in Fig. 2(a). Note that for the phase velocity-dependent superprism effect, the output PC/Si interface is rotated 90° with respect to the input Si/PC interface [see Fig. 2(a)]. Fig. 2(b) illustrates the refraction of light using the dispersion surfaces at the Si/PC interface, and Fig. 2(c) illustrates refraction at the PC/Si interface. The grey and black arrows in Fig. 2(b) represent \mathbf{k} -vectors for two different input beams which differ by only a small angle ($\Delta\theta_{\text{IN}} = 0.79^\circ$). As light propagates from silicon into the photonic crystal, the \mathbf{k} -vectors move from the circular uniform silicon dispersion surface to the square-shaped photonic crystal dispersion surface. At the Si/PC interface, the tangential component of the

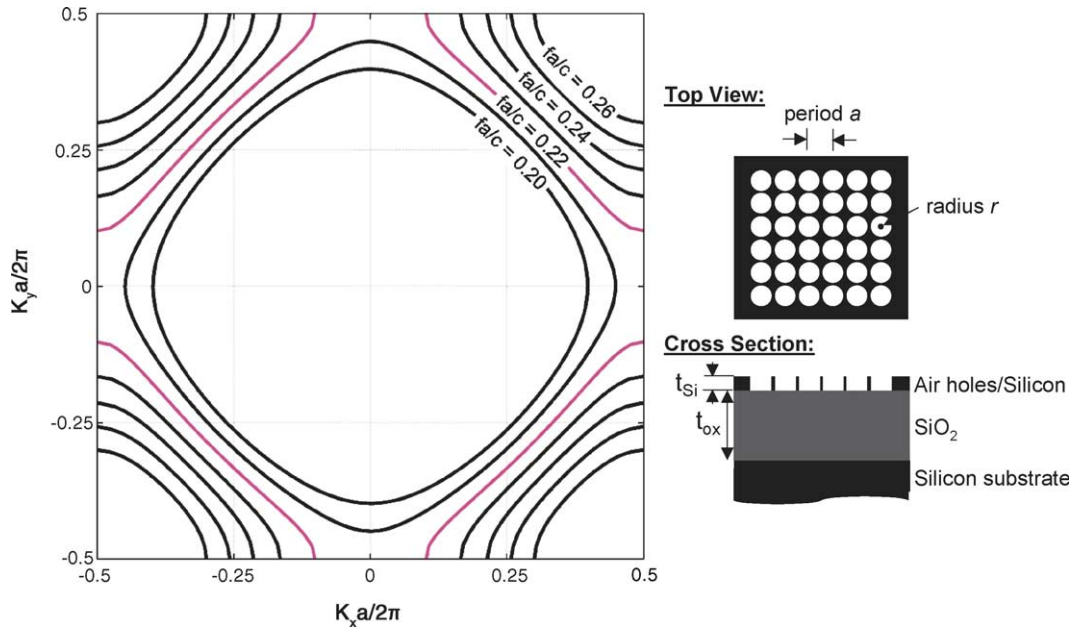


Fig. 1. Three-dimensional dispersion surface calculations for the even mode (TE-like; electric field mostly in the plane of the slab) of a 2D-periodic photonic crystal slab. Efficient superprism behavior is enabled by the “flatness” of the dispersion surfaces over large parameter regimes in k -space.

incident \mathbf{k} -vector must be conserved as the beam propagates into the photonic crystal (illustrated by the dash-dotted construction line which is a line of constant tangential \mathbf{k}). The intersection of the construction line with the photonic crystal dispersion curve determines the \mathbf{k} -vector within the photonic crystal. The small angular difference between the two input wavevectors translates into a large change in the normal component of the wavevector inside the photonic crystal due to the flatness of the dispersion surface (tangential \mathbf{k} is conserved). The two beams then travel toward the output interface of the photonic crystal with the energy propagating in the direction of the group velocity ($\mathbf{v}_g = \nabla_{\mathbf{k}}\omega$) as shown in Fig. 2(b). In the designed structure, the output interface is rotated by 90° with respect to the input interface [Fig. 2(a)] so that the large difference in the normal component of the \mathbf{k} -vector introduced at the input, results in a large difference in the tangential \mathbf{k} -vector at the output. With the tangential \mathbf{k} -vector conserved as the beam propagates out of the photonic crystal, the two beams now travel in different directions within the uniform silicon slab [Fig. 2(c)]. The result is a large angular change at the output of the photonic crystal for a very

small angular difference at the input of the photonic crystal. For example, with $fa/c = 0.22$, changing the input angle from $\theta_{IN} = 39.11^\circ$ to 38.31° ($\Delta\theta = 0.80^\circ$) will result in the output angle shifting from $\theta_{OUT} = 0^\circ$ to $\theta_{OUT} = 18.40^\circ$, implying an angular magnification factor $\Delta\theta_{OUT}/\Delta\theta_{IN} \approx 23$. All angles are defined with respect to the normal at the boundary.

Because the process implemented for fabricating the superprism structure can result in holes with a square shape, dispersion surface calculations were repeated for a structure with square-shaped holes of equal area to the circular holes discussed above (i.e. squares of width $d = 0.71a$). At a 5% higher frequency, the calculated dispersion surfaces for square holes closely resemble the dispersion surfaces for circular holes. More specifically, for the circular hole structure, the dispersion surface at the normalized frequency of $fa/c = 0.22$ closely resembles the dispersion surface at $fa/c = 0.22 \times 1.05$ for the structure with square-shaped holes. Operating a superprism with square-shaped holes at a frequency of $fa/c = 0.22$, would imply that the angular magnification is $\Delta\theta_{OUT}/\Delta\theta_{IN} \approx 15.5$ ($\theta_{IN} = 36.90^\circ$ – 36.10° , $\theta_{OUT} = 0^\circ$ – 12.43°). Changing the frequency of operation to $fa/c = 0.22 \times 1.05$

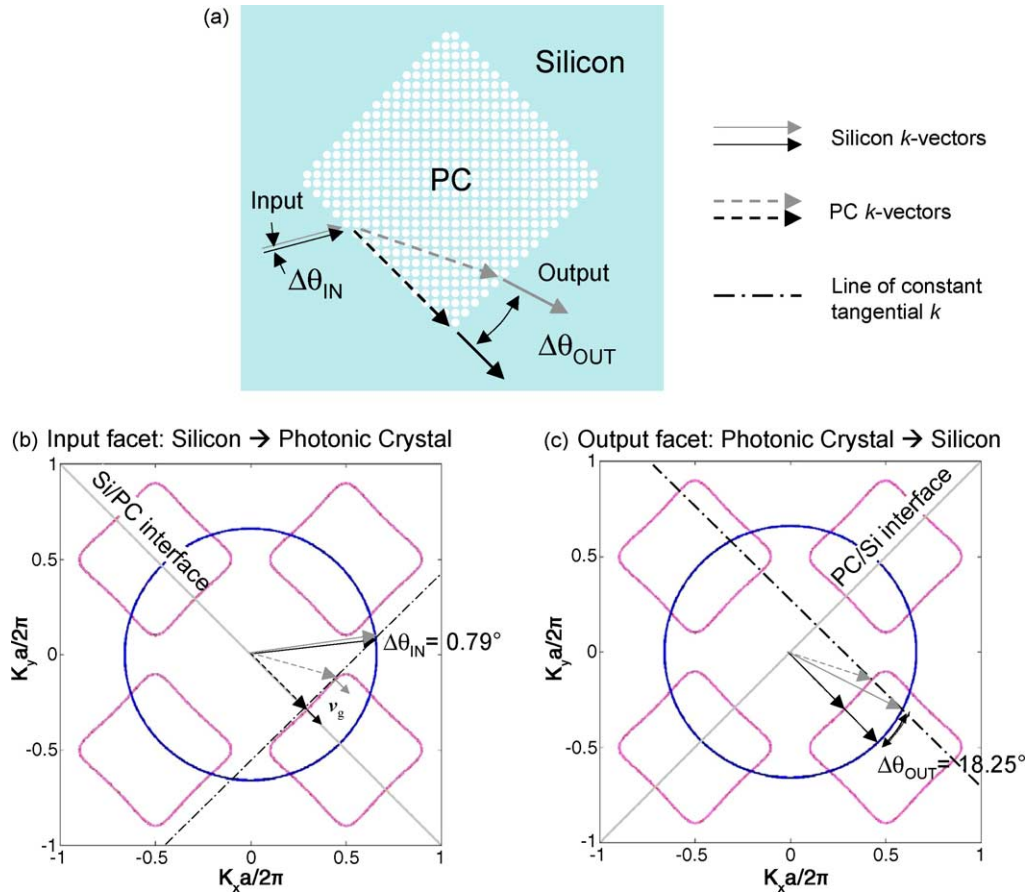


Fig. 2. Schematic illustrating the mechanism for superprism angular magnification using the dispersion surfaces of silicon and the photonic crystal. (a) The light path through the full superprism structure. (b) Coupling into the photonic crystal from silicon. (c) Coupling out of the photonic crystal into silicon. Note that the dash-dotted lines in (b) and (c) represent lines of constant tangential k .

would improve the magnification factor to $\Delta\theta_{OUT}/\Delta\theta_{IN} \approx 23$ —which is equivalent to the performance of the structure with circular holes.

The phase velocity effect can also be explored for realizing the superprism effect outside of the dielectric slab in air. As illustrated in Fig. 3, input and output facets can be defined as air-silicon boundaries positioned at specific angles (θ_1, θ_2) with respect to the photonic crystal edge. The orientation of these facets with respect to the photonic crystal edge can be designed such that light entering the input facet at near normal incidence, then exits the output facet at larger angles centered about the normal direction. The silicon regions thus act as conventional prisms to facilitate coupling to the photonic crystal from air at the appropriate angle for superprism action.

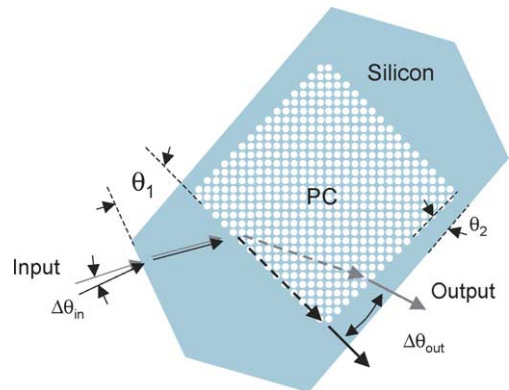


Fig. 3. Schematic illustrating a superprism structure for use in free space applications.

Computations

To demonstrate the feasibility of the phase velocity-dependent superprism effect, finite-difference time-domain simulations were performed on a simplified, more numerically tractable two-dimensional (2D) model. The simplified system has a square lattice photonic crystal of lattice constant a , circular air holes with radius $r = 0.35a$, and dielectric constant $\epsilon = 12$, but is purely 2D, assuming infinite structure thickness. The dispersion curves of the 2D system were calculated and were found to be similar to those of the 3D case that was presented in Fig. 1, but with small quantitative differences which result in an optimal operating frequency of $fa/c = 0.17$. At this frequency, changing the input angle for the structure described in Fig. 2 from $\theta_{IN} = 46.41^\circ$ to 44.56° will result in the output angle swinging from $\theta_{OUT} = 0^\circ$ to 24.92° for an angular magnification of $\Delta\theta_{OUT}/\Delta\theta_{IN} = 13.47$.

In the simulation shown in Fig. 4, a single frequency ($fa/c = 0.17$) Gaussian beam [$I \propto \exp(-2r^2/w_{Si}^2)$, where $w_{Si} = 73.12a$] is launched within the high index

silicon region ($\epsilon = 12$), propagates into the photonic crystal, and then exits into air ($\epsilon = 1$). Fig. 4(a) through (c) show the time evolution of the z component of the magnetic field distribution for three slightly different angles, θ_{IN} ($46.2 \pm 0.7^\circ$). All simulations are performed with a numerical spatial resolution of 20 pts/ a with a simulation area of $450a \times 50a$. The arrows within the figures serve as guides to the eye demonstrating how the direction of the beam shifts for a slight change in the input angle. Also, notice that the width of the magnetic field distribution in the photonic crystal is narrow ($w_{PC} \sim 15a$) and fairly constant for small input variations. In each of these cases, [Fig. 4(a–c)], the total transmitted output power was approximately one quarter of the input power. The remaining power was lost in two forms: (1) insertion loss due to reflection at the photonic crystal's input facet, and (2) power internally reflected within the photonic crystal at the output facet. In all cases of the simulation, internal reflection from the output facet then experiences subsequent reflections within the photonic crystal.

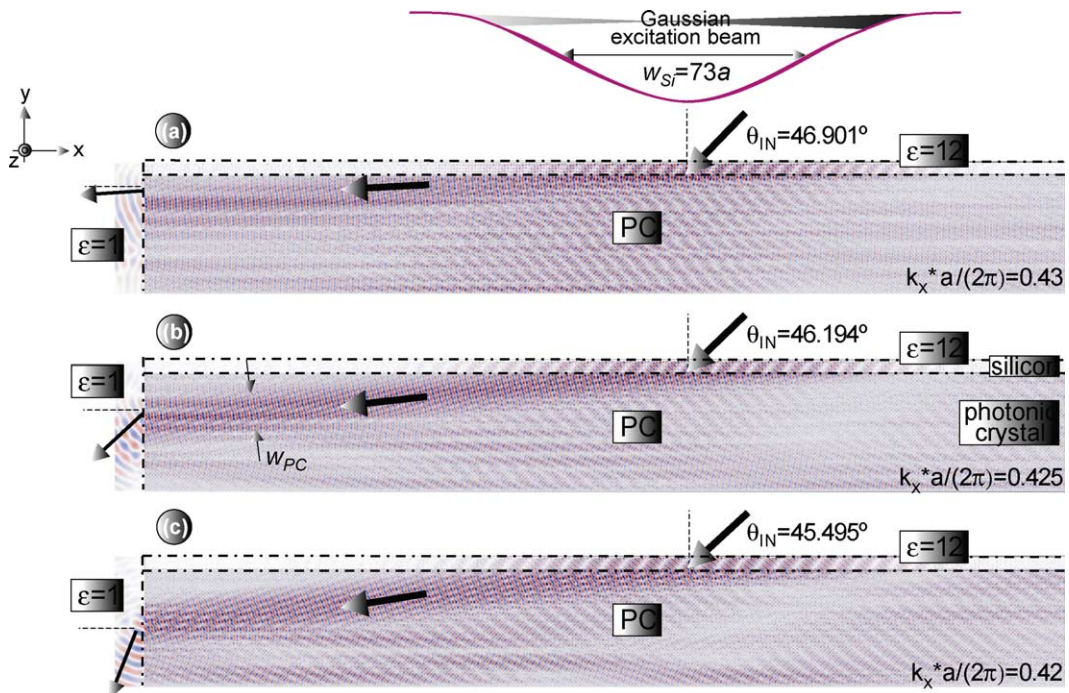


Fig. 4. Finite difference time domain simulation of a simplified 2D model of the structure simulated in Fig. 1. All cases (a) through (c) are calculated with a normalized frequency of $fa/c = 0.17$, with the electric field in the plane. Propagation of light from silicon ($\epsilon = 12$), through the photonic crystal, into air ($\epsilon = 1$) is shown. All angles are measured with respect to the normal direction.

Since the output beam in air, shown in Fig. 4, is excited with a narrow beam within the photonic crystal ($w_{PC} \sim 15a$), the output beam is divergent, implying that it is composed of a range of \mathbf{k} -vectors. With a divergent output beam, observation of the superprism effect becomes difficult to resolve. To broaden the propagating light within the PC and lessen its divergence, a wide excitation beam with a minimal range of \mathbf{k} -vectors is necessary. In other words, because a superprism is inherently sensitive to differences in \mathbf{k} , the excitation beam should approximate a plane wave (i.e. a single \mathbf{k} -vector) if the superprism effect is to be clearly resolved. A 2D simulation with a very broad excitation is computa-

tionally intensive. Nevertheless, the simulated behavior of light demonstrated in Fig. 4 indicates that when a broad excitation beam is used, a large area PC is required.

3. Experimental

A technique for fabricating the superprism structure with a large area photonic crystal has been explored. The structure consists of a two-dimensional photonic crystal slab with a square lattice of air holes in high index material. As shown in Fig. 5(a), the photonic crystal slab occupies a $1\text{ cm} \times 1\text{ cm}$ square

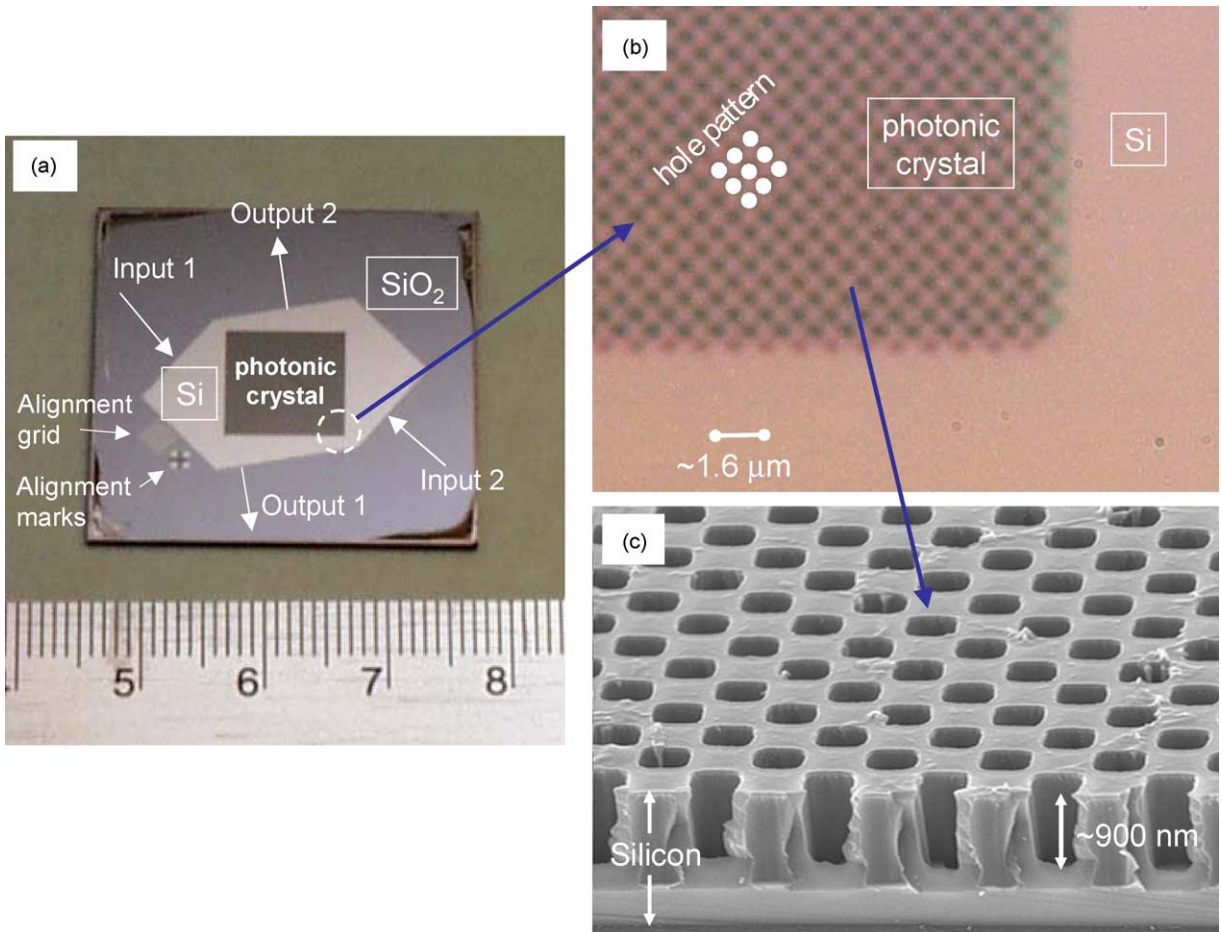


Fig. 5. Images of a fabricated superprism structure. (a) Digital photograph showing the full sample. (b) Differential interference contrast image showing the magnified corner area of the photonic crystal. (c) SEM micrograph showing cross-sectional image of a Si monitor sample.

area and rests on a low index SiO₂ layer. SOI (silicon on insulator) wafers purchased from Soitec, Inc. were used for this structure. The geometrical parameters (i.e. lattice constant, slat thickness, hole radius, etc.) of the fabricated photonic crystal were chosen to be compatible with a wavelength of 3.4 μm, with a silicon thickness of 700 nm, a SiO₂ thickness of 3000 nm, a photonic crystal lattice constant of 750 nm, and a hole radius of 300 nm. (Geometrical parameters for operation at a different wavelength would need to be appropriately scaled.) The input and output facets of the structure are air-silicon boundaries positioned at specific angles with respect to the photonic crystal to facilitate coupling from air as illustrated in Fig. 3. For this structure, the input angle (θ_1) was 38°, and the output angle (θ_2) was 11° as measured from the input and output Si/PC interfaces respectively. Calculations indicate that for this structure, an angular swing of $\pm 2^\circ$ about the normal at the input results in a $\pm 30^\circ$ swing about the normal at the output.

The high index region with the input and output facets was patterned using photolithography leaving an open square area for the subsequent patterning of the photonic crystal. The large area photonic crystal was patterned using two-beam interference lithography (IL) with a 325 nm wavelength HeCd laser. The photonic crystal grid is patterned using two IL exposures rotated by 90°. Patterning holes using this technique results in square rather than circularly shaped holes for large hole diameters. As a result, the size of the holes was adjusted to maintain the same air/silicon ratio as the design. Alignment of the photonic crystal to the open square area, mentioned above, was accomplished by using a 6 μm period alignment grid which was simultaneously patterned with the high index region during the photolithography step. The orientation of the alignment grid coincides with the desired orientation of the photonic crystal. Using the diffraction pattern formed by a 633 nm HeNe laser reflecting off the alignment grid, the sample was rotated until the axis of the IL exposure from the HeCd laser, was aligned to the axis of the diffraction pattern formed by the HeNe laser. With this technique, alignment of the photonic crystal to the boundary of the high index region, as illustrated in Fig. 5(b), was accomplished with angular precision of approximately 1 μm radian as

measured with a scanning electron microscope (SEM). An additional photolithography step was then used to protect the photonic crystal in order to remove the holes patterned outside of the square photonic crystal region during the IL step. Reactive ion etching was used to transfer the superprism pattern into a SiO₂ hard mask layer and then into the top silicon layer of the SOI layered structure. The cross-sectional profile of the photonic crystal in a silicon monitor sample after reactive ion etching is shown in Fig. 5(c). Fabricating the structure for an operating wavelength of $\lambda = 1.55 \mu\text{m}$ would proceed in the same fashion as described above but with smaller feature sizes.

4. Conclusion

A new structure to realize the superprism effect in uniform dielectric materials has been introduced. The structure relies on phase velocity sensitivity in a 2D photonic crystal slab to observe angular magnification outside the photonic crystal medium. Using three-dimensional equi-frequency calculations, the phase velocity superprism effect has been predicted for a photonic crystal slab of finite thickness. Calculations illustrate that a dispersion surface with a flat shape is ideal for introducing large changes in the phase velocity. Though the superprism effect can be observed in uniform dielectric materials, free space applications using a modified structure are also explored. Further analysis with finite-difference time-domain simulations indicate that for the clear observation of the superprism effect, a large area photonic crystal and a wide excitation beam is required. A fabrication technique is demonstrated to achieve the required nanometer-sized features of the structure over centimeter-scale areas using a combination of interference lithography, photolithography, and reactive ion etching with silicon-on-insulator substrates.

References

- [1] H. Kosaka, T. Kawashima, A. Tomita, M. Notomi, T. Tamamura, T. Sato, S. Kawakami, *J. Lightwave Tech.* 17 (1999) 2032.

- [2] H. Kosaka, T. Kawashima, A. Tomita, M. Notomi, T. Tamamura, T. Sato, S. Kawakami, *Appl. Phys. Lett.* 74 (1999) 1212.
- [3] B.E. Nelson, M. Gerken, D.A. Miller, R. Piestun, *Opt. Lett.* 25 (2000) 1502.
- [4] L. Wu, M. Mazilu, T. Karle, T.F. Krauss, *IEEE J. Quant. Elect.* 38 (2002) 915.
- [5] A. Lupu, E. Cassan, S. Laval, L. El Melhaoui, P. Lyan, J.M. Fedeli, *Opt. Exp.* 12 (2004) 5690.
- [6] S.G. Johnson, J.D. Joannopoulos, *Opt. Exp.* 8 (2001) 173.
- [7] For a review, see A. Taflove, *Computational Electrodynamics: The Finite-Difference Time-Domain Method*, Artech House, Norwood, Massachusetts, 1995.
- [8] C. Luo, M. Soljacic, J.D. Joannopoulos, *Opt. Lett.* 29 (2004) 745.
- [9] T. Baba, T. Matsumoto, M. Echizen, *Opt. Exp.* 12 (2004) 4608.